Full Articles

Redox potentials of iron—nitrosyl complexes: DFT calculations

N. S. Emel´yanova, A. F. Shestakov, and N. A. Sanina*

Institute of Problems of Chemical Physics, Russian Academy of Sciences,
1 prosp. Akad. Semenova, 142432 Chernogolovka, Moscow Region, Russian Federation.
Fax: +7 (496) 515 5420. E-mail: n_emel@mail.ru

Quantum chemical calculations of the structure and solvation energies of mono- and dianions of Roussin´s red salt esters $[Fe_2(\mu\text{-}RS)_2(NO)_4]$ (R = Me, Et, Pr^i, Bu^t) in solutions in THF and acetonitrile were carried out. In monoanions, an additional electron is localized on one $Fe(NO)_2$ fragment, which leads to significant structural distortion of the anion compared to neutral molecule. The second electron is localized on the other $Fe(NO)_2$ fragment; this causes symmetrization of the dianion geometry. There are good linear correlations between the calculated and experimental redox potentials of these systems. A relationship was proposed for estimation of the redox potentials of related iron—nitrosyl complexes. The standard redox potentials of the complex with R = Ph in water, DMSO, and acetonitrile evaluated using this expression lie between –0.5 and –0.6 V.

Key words: dinitrosyl iron complexes, NO donors, redox potentials, density functional theory, B3LYP functional.

Numerous studies showed that nitrogen monoxide molecule plays an important role in many biological processes.[1—4] It reacts with thiols and metal centers of proteins and controls various physiological processes. Dinitrosyl iron complexes (DNIC) and nitrosothiols are two possible forms for storage and transportation of nitrogen monoxide in biological systems. To study the functions of DNIC, the structures and reactivities of synthetic iron—nitrosyl complexes are intensively studied at present by a variety of methods including quantum chemical ones.[5—8]

The use of theoretical methods is particularly topical because of the difficulties in formal description of the electronic structure of DNIC. This is reflected in modern chemical nomenclature[9] where one should explicitly show the total number of valence electrons (n) on the coordination site bearing NO ligands, *e.g.*, $Fe(NO)_2^{[n]}$.

Decomposition products of DNIC include NO and N_2O, which indicates the formation of an ionic form NO^- or its protonated form HNO as intermediates. The redox reaction of NO^- with the starting binuclear iron complex may have a dual effect on the chemical dynamics of the process. On the one hand, the ionic form NO^- (N_2O precursor in the subsequent reactions) disappears. On the other hand, the reduced form of the DNIC is formed, which can differ in its NO-donor ability from the neutral form.

Published in Russian in *Izvestiya Akademii Nauk. Seriya Khimicheskaya,* No. 7, pp. 1329—1333, July, 2011.

1066-5285/11/6007-1352

An important role of redox processes in the DNIC decomposition is indirectly demonstrated by an increase in the NO yield under aerobic conditions compared to anaerobic conditions.[10] Therefore, the development of a theoretical approach to the determination of the redox potentials of the DNIC that control the thermodynamics of redox processes is undoubtedly interesting. This will allow one to analyze the mechanisms of the reactions involving complexes whose redox potentials are unknown.

Experimentally, redox processes have been quite well studied for Roussin´s red salt esters $[Fe_2(\mu\text{-}RS)_2(NO)_4]$ with alkyl substituents (binuclear forms of DNIC)[11—14] and for their reduced paramagnetic complexes $[Fe_2(\mu\text{-}RS)_2(NO)_4]^-$ and $[Fe_2(\mu\text{-}RS)_2(NO)_4]^{2-}$.[15—19] We studied the applicability of the density functional theory (DFT) to calculations of the redox potentials of this class of compounds and the possibility of introducing empirical corrections in order to improve the accuracy of theoretical predictions.

Calculation Procedure

To study the processes occurring in the reduction of complexes, we calculated the molecular and electronic structures of the mono- and dianions of Roussin´s red salt esters $[Fe_2(\mu\text{-}RS)_2(NO)_4]$ (R = Me, Et, Pr^i, Bu^t) and the redox potentials in solutions in THF and acetonitrile. Calculations were carried out using the Gaussian 98 program.[20] The geometries in different charged states with broken symmetry were optimized by the B3LYP/6-31G* method. The solvation energies were taken into account using the polarizable continuum model and the extended basis set 6-311++G**.

Results and Discussion

Molecular and electronic structures of anions of Roussin´s red salt esters $[Fe_2(\mu\text{-}RS)_2(NO)_4]$ (R = Me, Et, Pr^i, Bu^t). Previous studies of the complex with the phenyl substituent (R = Ph) showed (see, *e.g.*, Ref. 10) that the singlet broken-symmetry state has a distorted spin structure in which each iron atom bears three unpaired electrons with oppositely oriented spins (provided that the $Fe(NO)_2$ fragments have the local spin $S = 1/2$). This is indicated by both the spin population on the Fe atoms equal to about 2.4 and the average value of the squared total spin $\langle S^2 \rangle$, which equals half the theoretical value equal to five for the one-determinant function including n_a unpaired electrons with the spin α and n_b unpaired electrons with the spin β:

$$\langle S^2 \rangle = (n_a + n_b)/2 + (n_a - n_b)^2/4.$$

At the same time, the spin populations and $\langle S^2 \rangle$ values obtained for the open-shell systems were quite reasonable, as for the complexes with alkyl substituents studied in this work. As a consequence, consideration of the energy differences between the zero- and nonzero spin states faces some difficulties. Therefore, to minimize the systematic error, we used the energies of neutral complexes in the triplet state and those of the mono- and dianions with $S = 3/2$ and 1, respectively.

In the states with different total spins, the magnetic interactions between local spins in the binuclear complex are different, but this has little effect on the lengths of the valence bonds and on the bond angles. As an example, Fig. 1 shows the optimized structures of mono- and dianions for R = Et and indicates the excess electron density on the atoms. Table 1 lists the bond lengths in the $Fe(NO)_2$ fragments in the optimized structures of the neutral and charged complexes.

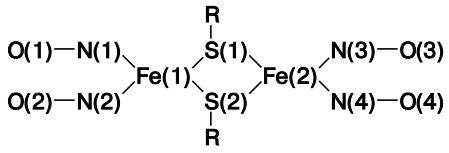

$[Fe_2(\mu\text{-}RS)_2(NO)_4]$

Slight elongation of N—O bonds compared to the bond lengths in the neutral complexes are different for two $Fe(NO)_2$ fragments (0.01 and 0.03—0.04 Å). The Fe—N distances remain almost unchanged on going to the charged complexes. The largest changes were found for the Fe—S distances which are almost equal in the initial compounds but lengthen in one fragment (to 0.3 Å, R = Et) and shorten by 0.02—0.04 Å in the other fragment of the asymmetric monoanions. This kind of structural distortion is due to nonuniform distribution of the negative charge in the monoanions (see Fig. 1), *viz.*, this charge is mainly localized on one $Fe(NO)_2$ fragment. This result is consistent with the conclusion drawn[19] based on experimental data.

The excess electron density is also distributed over the $Fe(NO)_2$ fragment nonuniformly, namely, it is to a greater extent localized on the oxygen atom of one of the two NO groups. In the gas phase, (see Fig. 1) the negative charge distribution is relatively more uniform; the effect of solvents (THF, acetonitrile) causes the polarization of the complex and the nonuniformity of the charge distribution to increase.

Consider transfer of an electron from one $Fe(NO)_2$ fragment to the other. The transition-state structure (see Fig. 1) is characterized by equal Fe—S distances and uniform charge distribution over the two $Fe(NO)_2$ fragments. The energy of this structure is only 1.8 kcal mol^{-1} higher than that of the ground-state structure (in the gas phase). In the dianion, the N—O distances further elongate compared to those in the neutral molecule. This suggests that extra electrons are localized on the antibonding π-orbitals of the NO ligand. As a consequence, the charge distribution becomes more uniform and the Fe—S distances become equalized. From Fig. 1 it follows that the second electron is mainly localized on the $Fe(NO)_2$

Table 1. Calculated bond lengths in neutral complexes $[Fe_2(\mu\text{-}RS)_2(NO)_4]$ (I) and in their anions (II)*

Bond	R = Me		R = Et			R = Pr^i			R = Bu^t	
	I	II (−1)	I	II (−1)	II (−2)	I	II (−1)	II (−2)	I	II (−1)
N(1)—O(1)	1.18	1.19	1.18	1.19	1.22	1.18	1.19	1.22	1.18	1.19
N(2)—O(2)	1.18	1.19	1.18	1.19	1.23	1.18	1.19	1.22	1.18	1.19
N(3)—O(3)	1.18	1.21	1.18	1.22	1.22	1.18	1.22	1.23	1.18	1.21
N(4)—O(4)	1.18	1.21	1.18	1.21	1.22	1.18	1.21	1.22	1.18	1.21
Fe(1)—N(1)	1.73	1.73	1.73	1.73	1.75	1.73	1.73	1.74	1.73	1.73
Fe(1)—N(2)	1.73	1.73	1.73	1.74	1.76	1.73	1.73	1.74	1.73	1.74
Fe(2)—N(3)	1.73	1.74	1.73	1.74	1.75	1.73	1.74	1.75	1.73	1.75
Fe(2)—N(4)	1.73	1.73	1.73	1.73	1.74	1.73	1.73	1.75	1.73	1.74
Fe(1)—S(1)	2.40	2.36	2.39	2.36	2.46	2.40	2.36	2.53	2.40	2.37
Fe(1)—S(2)	2.40	2.38	2.41	2.37	2.49	2.40	2.38	2.53	2.40	2.36
Fe(2)—S(1)	2.40	2.65	2.39	2.69	2.59	2.40	2.60	2.48	2.40	2.57
Fe(2)—S(2)	2.40	2.48	2.41	2.46	2.47	2.40	2.50	2.49	2.40	2.50

* The anion charges are given in parentheses.

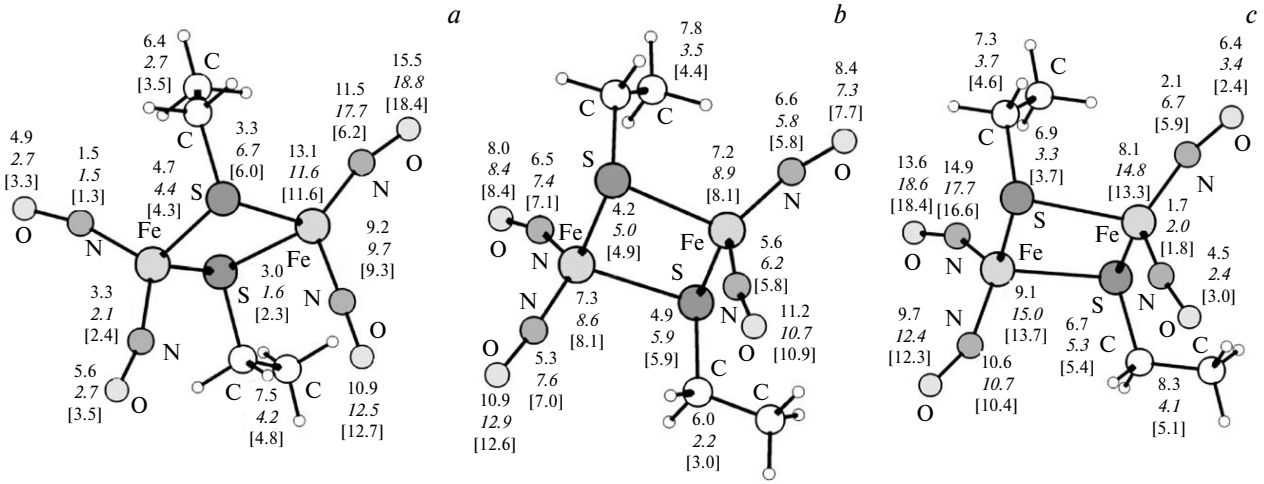

Fig. 1. Structures of mono- and dianions for R = Et: monoanion (*a*), transition state (*b*), and dianion (*c*). The relative electron density distribution compared to that in the neutral molecule is given near the atoms (roman type for the gas phase, in italic for acetonitrile, and in brackets for THF).

fragment that was depleted in electrons in the monoanion. Mention may also be made of some elongation of the Fe—N bonds.

Redox potentials. Calculations of the redox potentials of nitrosyl complexes in solutions are based on the thermodynamic cycle[21] (Scheme 1) relating the attachment of an electron in the condensed phase to the corresponding gas-phase process using the free energies of solvation of reactants and products.

In the gas phase, the role of the reduction potential is played by the electron affinity whose numerical values lie between —1.72 and —1.75 eV for the complexes in

Scheme 1

$$[Fe_2(\mu\text{-}RS)_2(NO_4)]\ (g) + e \xrightarrow{EA} [Fe_2(\mu\text{-}RS)_2(NO_4)]^-\ (g)$$

$$\Delta G_s^\circ[Fe_2(\mu\text{-}RS)_2(NO_4)] \downarrow \qquad \downarrow \Delta G_s^\circ = 0 \qquad \downarrow \Delta G_s^\circ[Fe_2(\mu\text{-}RS)_2(NO_4)]^-$$

$$[Fe_2(\mu\text{-}RS)_2(NO_4)]\ (s) + e \xrightarrow{V} [Fe_2(\mu\text{-}RS)_2(NO_4)]^-\ (s)$$

EA is the electron affinity, *V* is the redox potential

question. Since the standard redox potentials are given for $T = 298.15$ K, gas-phase free energy calculations should be performed taking into account the thermal and entropy contributions. However, free electrons are not actually involved in the reactions. Therefore, electron attachment (or abstraction) is treated as a step of the standard process of hydrogen formation from protons at a standard hydrogen electrode (SHE):

$$H^+(aq) + e(g) \longrightarrow 0.5\ H_2(g). \qquad (1)$$

This semireaction is used to calculate the redox potentials.

The standard free energy of reaction (1) determined from the totality of experimental and theoretical data[22] is −4.36 eV. The standard redox potential (in V) is thus given by

$$V^{n/n-1} = -\{G^\circ([Fe_2(SR)_2(NO)_4]^{n-1}) - G^\circ([Fe_2](SR)_2(NO)_4]^n\}/F + 4.36, \qquad (2)$$

where F is the Faraday constant and $G^\circ([Fe_2](SR)_2(NO)_4]^n)$ is the standard free energy of the complex $[Fe_2](SR)_2(NO)_4]^n$, which equals the sum of its total energy in the gas phase, the thermal correction for the Gibbs free energy, and the free energy of solvation. To compare the results obtained from calculations with experimental data, one should take into account the fact that they are usually reported in the literature relative to the potential of the redox transition in ferrocene ($[Cp_2Fe]^0$—$[Cp_2Fe]^+$) and conversion to the SHE requires subtraction of a value of 0.34 V from the experimental data.[15]

The results of calculations are compared with the experimental data[15] in Table 2. As can be seen, in all cases, for the transition 0→1 the theoretical values are more negative than the experimental ones. Specific trends are observed in this case (see Table 3). The differences between the experimental and theoretical redox potentials are nearly constant and decrease for acetonitrile and THF as the volume of the substituent R increases. These differences are somewhat larger for THF than for acetonitrile.

Table 2. The calculated and experimental (relative to SHE) redox potentials of complexes $[Fe_2(\mu\text{-}RS)_2(NO)_4]$

Substituent R	Solvent	−V/V			
		Calculations		Experiment[15]	
		0 → −1	−1 → −2	0 → −1	−1→ −2
Me	THF	1.187	—	0.710	1.530
	MeCN	0.999	—	0.595	1.255
Et	THF	1.178	1.420	0.734	1.532
	MeCN	0.988	0.903	0.612	1.270
Pr	CH_2Cl_2	1.127	—	0.820	—
Pr^i	THF	1.158	1.511	0.755	1.529
	MeCN	0.968	0.998	0.623	1.285
Bu^t	THF	1.152	—	0.778	1.485
	MeCN	0.948	—	0.635	1.240
	CH_2Cl_2	1.116	—	0.860	1.470
Ph	MeCN	0.907	—	—	—
	CH_2Cl_2	1.047	—	—	—
	DMSO	0.897	—	—	—
	H_2O	0.916	—	—	—

Table 3. Differences between the experimental and theoretical redox potentials of the complexes $[Fe_2(\mu\text{-}RS)_2(NO)_4]$ in THF and acetonitrile

Substituent R	ΔV/V	
	MeCN	THF
Me	0.404	0.477
Et	0.376	0.444
Pr^i	0.345	0.403
Bu^t	0.313	0.374

Figure 2 demonstrates that the calculated redox potentials of the complexes with the substituents R = $= CH_{3-n}Me_n$ (n = 0—3) show a good linear correlation with the experimental values for both solvents:

$$V^{exp}(MeCN) = -0.7357V^{calc}(MeCN) - 1.3341,$$

$$V^{exp}(THF) = -1.7192V^{calc}(THF) - 2.7536.$$

These correlation equations describe the experimental data to an accuracy of 0.005 V for acetonitrile and 0.008 V for THF.

This gives grounds to use these correlation equations for evaluating the redox potentials of other complexes. For instance, the estimates of the redox potentials of the complex with R = Pr are −1.174 V in THF and −0.974 V in acetonitrile. The corresponding experimental values are equal to −1.075 and −0.958 V, *i.e.*, the differences are 100 mV for THF and 16 mV for acetonitrile. Thus, the error in

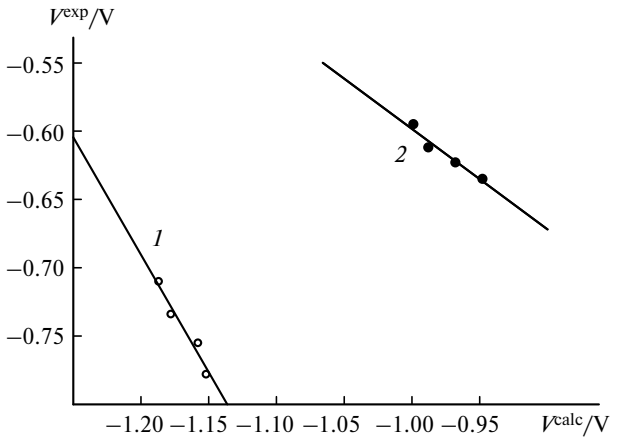

Fig. 2. Correlations between the theoretical and experimental redox potentials for THF (*1*) and MeCN (*2*) as solvents.

calculations of the redox potentials can be as high as 100 mV for other systems; this will be taken into account later.

Since the DNIC with the aromatic substituent R = Ph is thought to be a promising antitumor drug, it is of interest to evaluate its redox potential.[23] The calculated standard redox potential of the Roussin´s red salt ester $[Fe_2(\mu\text{-}PhS)_2(NO)_4]$ in acetonitrile is –0.907 V; using the correlation equation, one gets –0.67±0.10 or –1.01±0.10 V for the redox potential relative to the ferrocene—ferricinium transition used in the electrochemical experiments for these systems.[15,16]

Since correlations were obtained for alkyl substituents, they are probably less accurate for the complexes with substituents of other chemical structure. Therefore, we used the following approach. On the average, the estimated redox potentials differ from the experimental values by a value of 0.350 V for acetonitrile and 0.420 V for THF (see Table 3). Using these values as constants (a sort of correction), one gets somewhat different redox potentials of the complex $[Fe_2(\mu\text{-}PhS)_2(NO)_4]$. They are equal to –0.56 for acetonitrile and –0.66 V for THF with an estimated error of ±0.05 V. Since these corrections are rather close for different solvents, one can use a more rough correlation equation: $V^{exp} = V^{calc} + 0.4$ (V) with an error of ±0.1 V. In this case, the estimated redox potentials of the phenyl complex are –0.52±0.10 V in water, –0.50±0.1 V in DMSO, and –0.65±0.1 V in dichloromethane. Obtaining higher accuracy when extending the approach to other solvents requires experimental data for calibration; unfortunately, they are unavailable at the moment.

Thus, our quantum chemical calculations of mono- and dianions of Roussin´s red salt esters $[Fe_2(\mu\text{-}RS)_2(NO)_4]$ (R = Me, Et, Pr^i, Bu^t) in solutions in THF and acetonitrile showed that (i) these compounds form stable structures upon the attachment of one and two electrons and (ii) the first electron is localized on one $Fe(NO)_2$ fragment, which leads to significant distortion of the anion structure compared to neutral molecule. The second electron is localized on the $Fe(NO)_2$ fragment and causes symmetrization of the dianion geometry. The calculated redox potentials of the alkyl esters of Roussin´s red salt in THF and acetonitrile show good linear correlations with the corresponding experimental data. This allowed one to estimate the redox potentials of the phenyl ester for a number of solvents.

References

1. T. G. Traylorand, V. S. Sharma, *Biochemistry*, 1992, **31**, 2847.
2. T. S. Lai, A. Hausladen, T. F. Slaughter, J. P. Eu, J. S. Stamlerand, C. S. Greenberg, *Biochemistry*, 2001, **40**, 4904.
3. J. Huang, S. B. Hadimani, J. W. Rupon, S. K. Ballas, D. B. Kim-Shapiroand, S. B. King, *Biochemistry*, 2002, **41**, 2466.
4. R. Silaghi-Dumitrescu, D. M. Jr. Kurtz, L. G. Ljungdahland, W. N. Lanzilotta, *Biochemistry*, 2005, **44**, 6492.
5. M. Javorska, Z. Stasicka, *New J. Chem.*, 2005, **29**, 604.
6. L. Li, R. Wang, M. A. Camacho-Fernandez, W. Xu, J. Zhang, *J. Biol. Inorg. Chem*., 2009, **14** (Suppl.1), 132.
7. J. Conradie, D. A. Quarless, Jr. H.-F. Hsu, T. C. Harrop, S. J. Lippard, S. A. Koch, A. Ghosh, *J. Am. Chem. Soc.*, 2007, **128**, 10446.
8. I.-J. Hsu, C.-H. Hsieh, S.-C. Ke, K.-A. Chiang, J.-M. Lee, J.-M. Chen, L.-Y. Jang, G.-H. Lee, Y. Wang, W.-F. Liaw, *J. Am. Chem. Soc.*, 2007, **129**, 1151.
9. J. H. Enemark, R. D. Feltham, *Coord. Chem. Rev.*, 1974, **13**, 339.
10. N. A. Sanina, N. S. Emel´yanova, A. N. Chekhlov, A. F. Shestakov, I. V. Sulimenkov, S. M. Aldoshin, *Izv. Akad. Nauk*, *Ser. Khim.*, 2010, 1104 [*Russ. Chem. Bull., Int. Ed.*, 2010, **59**, 1126].
11. C. Glidewell, M. E. Hannan, M. B. Hursthouse, I. L. Johnsonand, M. Motevalli, *J. Chem. Res.*, 1988, **7**, 212.
12. T. W. Hayton, P. Legzdinsand, W. B. Sharp, *Chem. Rev.*, 2002, **102**, 935.
13. C.-Y. Chiang, M. L. Miller, J. H. Reibenspiesand, M. Y. Darensbourg, *J. Am. Chem. Soc.*, 2004, **126**, 10867.
14. T. C. Harrop, D. Song, S. J. Lippard, *J. Am. Chem. Soc.*, 2006, **128**, 3528.
15. J. A. Crayston, C. Glidewell, R. J. Lambert, *Polyhedron*, 1990, **9**, 1741.
16. R. Wang, M. A. Camacho-Fernandez, W. Xu, J. Zhangand, L. Li, *Trans. Faraday Soc., Dalton Trans.*, 2009, 777.
17. C. Glidewell, R. J. Lambert, *Polyhedron*, 1992, **11**, 2803.
18. C.-C. Tsou, T.-T. Lu, W.-F. Liaw, *J. Am. Chem. Soc.*, 2007, **129**, 12626.
19. T.-T. Lu, C.-C. Tsou, H.-W. Huang, I.-J. Hsu, J.-M. Chen, T.-S. Kuo, Y. Wang, W.-F. Liaw, *Inorg. Chem.*, 2008, **47**, 6040.
20. M. J. Frisch, G. W. Trucks, H. B. Schlegel, G. E. Scuseria, M. A. Robb, J. R. Cheeseman, V. G. Zakrzewski, J. A. Montgomery, Jr., R. E. Stratmann, J. C. Burant, S. Dapprich, J. M. Millam, A. D. Daniels, K. N. Kudin, M. C. Strain, O. Farkas, J. Tomasi, V. Barone, M. Cossi, R. Cammi, B. Mennucci, C. Pomelli, C. Adamo, S. Clifford, J. Ochterski, G. A. Petersson, P. Y. Ayala, Q. Cui, K. Morokuma, D. K. Malick, A. D. Rabuck, K. Raghavachari, J. B. Foresman, J. Cioslowski, J. V. Ortiz, A. G. Baboul, B. B. Stefanov, G. Liu, A. Liashenko, P. Piskorz, I. Komaromi, R. Gomperts, R. L. Martin, D. J. Fox, T. Keith, M. A. Al-Laham, C. Y. Peng, A. Nanayakkara, C. Gonzalez, M. Challacombe, P. M. W. Gill, B. Johnson, W. Chen, M. W. Wong, J. L. Andres, C. Gonzalez, M. Head-Gordon, E. S. Replogle, J. A. Pople, *Gaussian 98, Revision A.7*, Gaussian, Inc., Pittsburgh (PA), 1998.
21. P. Winget, C. J. Cramer, D. G. Truhlar, *Theor. Chem. Acc.*, 2004, **112**, 217.
22. T. R. Tuttle, S. Malaxos, J. V. Coe, *J. Phys. Chem.*, 2002, **106**, 925.
23. N. A. Sanina, O. S. Zhukova, Z. S. Smirnova, L. M. Borisova, M. P. Kiseleva, S. M. Aldoshin, *Ross. Bioterap. Zh.* [*Russ. Biotherap. J.*], 2008, No. 1, 52 (in Russian).

Received March 4, 2011;
in revised form June 10, 2011